Postprint of: Mohammed A., Golijanek-Jędrzejczyk A.: Estimating the uncertainty of discharge coefficient predicted for oblique side weir using Monte Carlo method FLOW MEASUREMENT AND INSTRUMENTATION Vol. 73 (2020), 101727
DOI:10.1016/j.flowmeasinst.2020.101727

Estimating the uncertainty of discharge coefficient predicted for oblique side weir using Monte Carlo method

Ahmed Y. Mohammed[1] and Anna Golijanek-Jędrzejczyk[2]

ahmedymaltaee@gmail.com ; a.altaee@uomosul.edu.iq and anna.golijanek-jedrzejczyk@pg.edu.pl
[1]Dams and Water Resources Engineering, College of Engineering, University of Mosul, Mosul, Iraq.
[2]Gdańsk University of Technology, Faculty of Electrical and Control Engineering, Gdańsk, Poland

Abstract:

Side weir is a hydraulic structure, which is used in irrigation systems to divert some water from main to side channel. It is installed at the entrance of the side channel to control and measure passing water into the side channel. Many studies provided side weir water surface profile and coefficient of discharge to measure water discharge diverted into the side channel. These studies dealt with different side weir shapes (rectangular, trapezoidal, triangular and circular), which were installed perpendicular to the flow direction. Recently, some studies dealt with skew side weir, but these studies still need to more investigation. Here we report to investigate oblique side weir theoretically using statistical method to supported other studies in this case. Measurement uncertainty discharge coefficient C_d was obtained by two methods: analytical according to the 'Guide to the expression of uncertainty in measurement' and the Monte Carlo method. The results indicate that all experimental results are consistent with the analytical results. The relative expanded uncertainty of the discharge coefficient C_d does not exceed 2%.
Keywords: oblique side weir; coefficient of discharge; Monte Carlo; open channel; side channel

1. Introduction:

Side weir is widely constructed at the side of the main channel. Therefore, water can pass over this side weir from main to side channel. The flow over this hydraulic structure system is complex, so many studies dealt with these phenomena since 1934 by DeMarchi [1]. The studies with different gaps related to the side weir, such as flow over different channel geometry of side weir (rectangular, triangular, trapezoidal and circular channels) [2-10]. Other studies deal with coefficient of discharge equation for side weir [11- 15]. Mwafaq and Ahmed [16] investigated discharge coefficient for inclined side crested weir, this study indicates increasing in discharge coefficient then increasing in discharge passing from main to side channel when increasing angle of inclined inside crest of side weir. Ahmed [17], Ahmed [18] and Ahmed et.al. [19] simulated flow over side weir using Simulink technic. Azza [20] presented the following equation for discharge coefficient for skew side weir turn to left and right according to water flow direction (Fig. 1) as shown in eq. (1) (when side weir turns to left) and eq.(2) (when side weir turns to right) respectively:

$$C_d = -2.38\, F_3^{0.057} \left(\frac{y3}{y1}\right)^{0.128} \left(\frac{L}{b}\right)^{-0.248} \quad (1)$$

$$C_d = -2.08\, F_3^{0.237} \left(\frac{y3}{y1}\right)^{0.294} \left(\frac{L}{b}\right)^{-0.238} \quad (2)$$

where C_d is coefficient of discharge, F_3 is Froude number in the side channel, y_3 and y_1 is water depth at side channel and upstream main channel respectively, L is the length of side weir crest and b is the width of side channel.

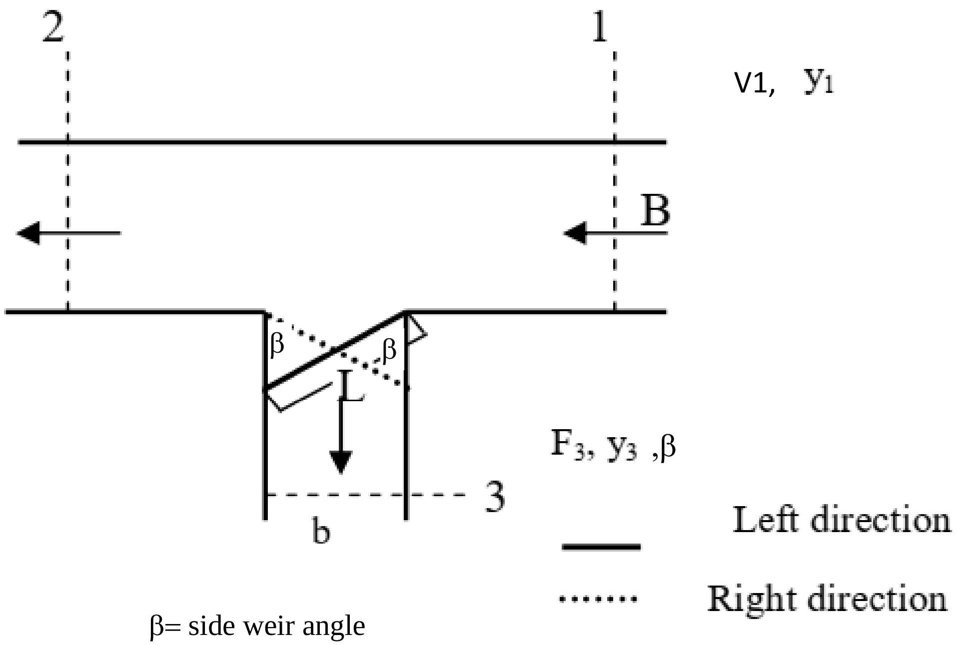

Fig. 1. Sketch of flow in a main and side channel with oblique side weir, [20].

Recently, Isa et.al. [21] presented new theoretical investigated for flow over side weir using new statistical program (Gene expression programming).

The Monte Carlo (MC) is a numerical tool, which generally simulates an unlimited number of unique measurements by random sampling from the known probability density function of all input quantities and propagates their distributions for the measurement model as the output. This method is used for simulations of different kinds of phenomena [26, 27]. Recently, it is often used in analyzes of the uncertainty of water flow, both in hydraulic installations [28, 29, 30] as well as in the analysis and prediction of water flow in rivers [31, 32, 33].

This article presents the results of uncertainty estimation of the discharge coefficient C_d for a side oblique weir installed inclined to the side channel. These uncertainty estimation was obtained by two methods: analytical according to the 'Guide to the expression of uncertainty in measurement' (GUM) [23,24] and the Monte Carlo method [25]. The first method is the method based on a convolution of the input distribution values, using a mathematical model. In this case, the designated measure of uncertainty is the expanded uncertainty, calculated as the product of the coverage factor k_p and the standard uncertainty value.

2. Experiments description

According to Azza [20] the experiments were conducted in the hydraulic laboratory of dams and water resources engineering at Mosul University. The object of research was a rectangular channel 10 m long, 0.3 m width and 0.45 m depth. The side flume was 2 m long, 0.15 width and 0.3 m depth. The discharge at the main channel was measured using standard weir installed at the end of the main channel.

The woody side weir has 12*15*0.1 cm dimensions installed at angles (30°, 45°, 60°, 75°, and 90°) with respect to the side channel (inclined to the left). Five different discharges with a total of 45 experiments were done. The water surface profile (water depths) in the main channel upstream and downstream side weir are measured as well as the water depths in the side channel and discharges were measured (Fig. 2).

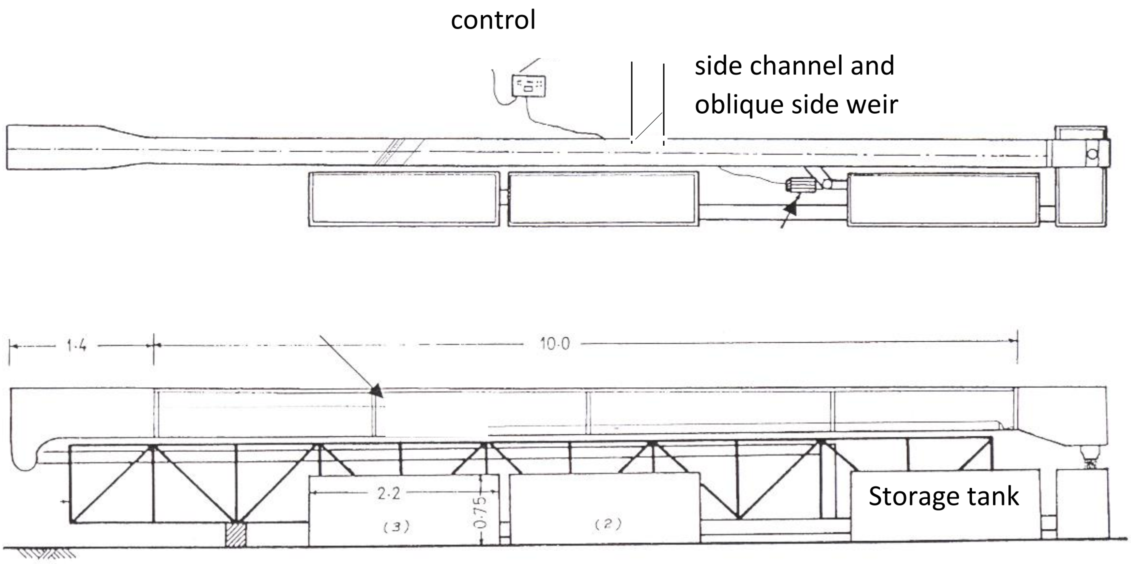

Fig. 2. Sketch of the hydraulic laboratory.

The ranges of various parameters are given in Table 1.

Table 1. Range of parameters measured for different cases.

P [cm]	**C_d [-]**	**Q_1 [l/s]**	**Q_2 [l/s]**	**Q_3 [l/s]**	**F_1 [-]**	**V_1 [m/s]**	**L/b [-]**	**p/y_1 [-]**	**β [rad]**	**y_1 [cm]**	**L [cm]**
10	0.65-0.82	7.2-18.4	6.8-16.0	0.4-2.4	0.11-0.18	0.14-0.26	1-2	0.57-0.68	1.75-0.52	0.17-0.2	0.15-0.3

3. Methodology for Determining the Discharge Coefficient

The Monte Carlo method is used to verify the estimates of analytical uncertainty, especially in the cases when the researcher deals with an indirect measurement of the measured value and when the measuring function is non-linear.

The first step of the Monte Carlo algorithm is a selection of the number *M* of the trials and generation of *M* vectors by random sampling from the probability density function for the (set of *N*) input quantities.

The next step in the procedure the MC is the evaluation of the model to give the corresponding output quantity and estimation of the output of the model. Then it should be sorted the model values into non-decreasing order. The last stage is to use of the sorted values to estimate the uncertainty for the output.

To understand the theoretical basis of flow over the side weir, DeMarchi [1] assumed a general expression for the water surface profile along the side weir derived by making use of energy relationships on the basis of the constant specific energy as in the theoretical analysis.

The specific energy *E* of the flow is:

$$E = y + \frac{v^2}{2g} \qquad (3)$$

where, *y*-water depth, *v*- mean velocity and *g*- acceleration due to gravity.

Equation (3) can be also written as:

$$E = y + \frac{Q^2}{2gA^2} \qquad (4)$$

where *Q* - flow discharge, and *A* – cross-section area of flow, channel width (*B*) by water depth (*y*) = (*B***y*).

Then from eq. (4) flow discharge *Q* can be fined as:

$$Q = By\sqrt{2g(E-y)} \qquad (5)$$

For side channel the discharge *Q* varies with distance along the main channel *x*, that is why the equation of a convened weir assumed for discharge per unit length *q* as:

$$q = -\frac{dy}{dx} = \frac{2}{3}C_d\sqrt{2g}(E-P)^{3/2} \qquad (6)$$

where *P*- weir height.

4. Dimensional analysis

Discharge coefficient for an oblique side weir can be defined as a function of some variables influence on flow such as upstream velocity (v_1), upstream water depth (y_1), acceleration due to gravity (*g*), side weir crest length (*L*), side channel width (*b*), side weir crest height (*P*), dynamic viscosity of water (μ), density of water (ρ), and side weir angle with respect to side channel (β)

$$C_d = f(V_1, y_1, g, L, b, P, \mu, \rho, \beta) \qquad (7)$$

Applying Buckingham theorem, the above equation can be written as a non-dimensional equation in the following form:

$$C_d = f(\frac{V_1}{\sqrt{gy1}}, \frac{L}{y1}, \frac{b}{y1}, \frac{P}{y1}, \frac{\mu}{\rho V1L}, \beta) \qquad (8)$$

where, upstream Froude number $F_1 = \frac{V_1}{\sqrt{gy1}}$, Reynold's number $1/R = \frac{\mu}{\rho V1L}$ and this can be neglected in open channel flow, the variables $\frac{L}{y1}$ and $\frac{b}{y1}$ can be reduced to $\frac{L}{b}$ by multiplying and rectification, so the eq. (8) can be written as the function of the following parameters:

$$C_d = f(F1, \frac{L}{b}, \frac{P}{y1}, \beta) \qquad (9)$$

The discharge coefficient for a side weir was defined as (actual to theoretical discharge) [1], according to [18], eq. (9) can be written as:

$$C_d = 1.275 - 0.619\frac{v_1}{\sqrt{gy_1}} - 0.522\frac{p}{y_1} + 0.028\frac{L}{b} - 0.132\beta \qquad (10)$$

The discharge coefficient C_d is determined indirectly, and the function of the measurement is dependent on the following parameters: $C_d = f(v_1, y_1, p, L, b, \beta)$.

5. Results and Discussion

5.1 Determination of the Uncertainty of the Discharge Coefficient Measurement

5.1.1. Analysis of the measurement uncertainty according to GUM

The analytical method for determining the uncertainty of discharge coefficient measurement is presented below.

Complex uncertainty $u_c(C_d)$ determining the mass flow q is defined as follows [23, 24]:

$$u_C(C_d) = \sqrt{u_A^2(C_d) + u_B^2(C_d)} \qquad (11)$$

where: $u_A(C_d)$ – is uncertainty Type A, and $u_B(C_d)$ – is uncertainty Type B.

The standard uncertainty $u_A(C_d)$ of the measurement is evaluated as [23, 24]:

$$u_A(C_d) = \sqrt{\frac{\sum_{i=1}^{n}(C_{di} - \overline{C_d})^2}{n(n-1)}} \qquad (12)$$

where:

n - number of C_d measurements,

C_{di} - the measured C_d value for i =1, 2, …n,

$\overline{C_d}$ - C_d arithmetic mean value.

Assuming no correlation between the uncertainties of measured quantities, according to the law of the uncertainty propagation [23, 24], the one of Type B determining the discharge coefficient C_d is defined as follows:

$$u_B(C_d) = \sqrt{{c_0}^2u^2(v_1) + {c_1}^2u^2(y_1) + {c_2}^2u^2(p) + {c_3}^2u^2(L) + {c_4}^2u^2(b) + {c_5}^2u^2(^{\beta})} =$$
$$= \sqrt{\left(\frac{\partial C_d}{\partial v_1}\right)^2 u^2(v_1) + \left(\frac{\partial C_d}{\partial y_1}\right)^2 u^2(y_1) + \left(\frac{\partial C_d}{\partial p}\right)^2 u^2(p) + \left(\frac{\partial C_d}{\partial L}\right)^2 u^2(L) + \left(\frac{\partial C_d}{\partial b}\right)^2 u^2(b) + \left(\frac{\partial C_d}{\partial ^{\beta}}\right)^2 u^2(^{\beta})}$$
(13)

where c_0 to c_5 marks sensitivity coefficients.

There are defined in Table 2.

Table 2. The weight coefficients arranged to equation (4) (partial derivatives).

Partial derivatives	**Formula**	
$c_0\left[\frac{s}{m}\right]$	$\frac{-0.619}{\sqrt{gy_1}}$	(14)
$c_1\left[\frac{1}{m}\right]$	$\frac{0.3095v_1}{\sqrt{gy_1^3}} + \frac{0.522p}{y_1^2}$	(15)
$c_2\left[\frac{1}{m}\right]$	$\frac{-0.522}{y_1}$	(16)
$c_3\left[\frac{1}{m}\right]$	$\frac{0.028}{b}$	(17)
$c_4\left[\frac{1}{m}\right]$	$\frac{-0.028L}{b^2}$	(18)
$c_5[-]$	-0.132	(19)

The variance values (from Table 3) were determined as Type B uncertainty variance from the following formula:

$$u^2 = \left(\frac{\Delta_{max}}{\sqrt{3}}\right)^2 \qquad (20)$$

The variances u2(V1) and u2(b) was determined assuming a rectangular distribution of error probability of measuring these parameters. The maximum error Dmax of measurement the velocity V1 and angle b was 0.1 mm. The velocity was measured using the Pitot tube tool, this device has ruler. Its accuracy was 0.1mm. The angle b was measured directly using protractor and triangles with ruler and its accuracy was equal 0.1 mm. The maximum error Dmax of the following parameters: upstream main channel y1, the length of the side weir crest L, the width of side channel b, the height of side weir p was 0.01mm.

Table 3. The values of the partial variances.

Variance	Distribution	Value [$\cdot 10^{-9}$]
$u^2(\nu_1)$ $\left[\frac{m^2}{s^2}\right]$	Rectangular	3.33
$u^2(y_1)$ $[m^2]$		$3.33\cdot10^{-2}$
$u^2(p)$ $[m^2]$		$3.33\cdot10^{-2}$
$u^2(L)$ $[m^2]$		$3.33\cdot10^{-2}$
$u^2(b)$ $[m^2]$		$3.33\cdot10^{-2}$
$u^2(\beta)$ $[-]$		3.33

Finally, the combined standard uncertainty $u_c(C_d)$ can be determined from the formula (11).

The expanded uncertainty of discharge coefficient $U_p(C_d)$ measurement for the coverage factor k_p = 2.01 (which corresponds to approximately 95% probability of expansion for normal distribution) is:

$$U_p(C_d) = 2.01 \cdot u_c(C_d) \tag{21}$$

In conclusion, the final result can be written as:

$$\overline{C_d} \pm U_p(C_d)$$

5.1.2. Analysis of the measurement uncertainty using the Monte Carlo method

Monte Carlo simulation was performed to verify the results of the estimated uncertainty that were obtained, this simulation was conducted with the same assumptions and for the same formulas as for the analytical method.

Estimation of uncertainty using Monte Carlo was performed in Microsoft Excel for the number of samples M equal to 10^4. The value of the expected discharge coefficient C_d and its density function for a confidence level equals 95% and $k_p = 2.01$ was determined and applied to the following presentation.

Figure 5 shows the probability density function of the simulated numerical values of discharge coefficient C_d for β =1.57 rad.

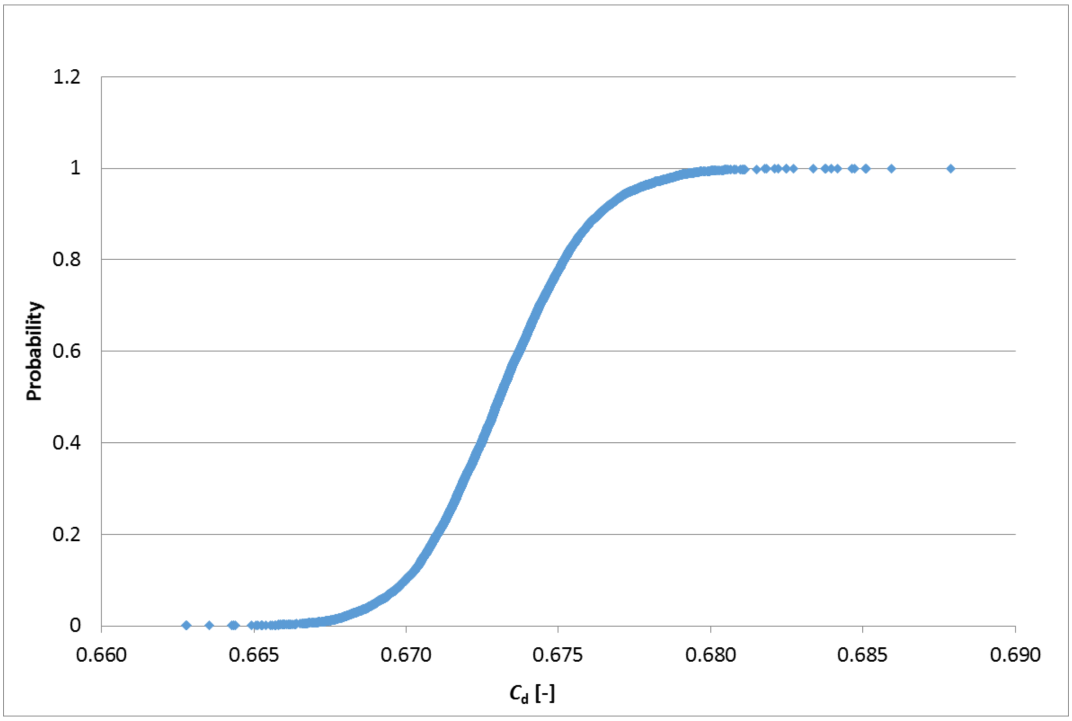

Fig. 5. Simulation of the outflow distribution of the discharge coefficient $C_d = 0.673$.

Based on these results, a histogram established with channel 0.3.10-3 (understood as the bin, calculated as the spread of measurements divided by the number of bins) was plotted in Figure below.

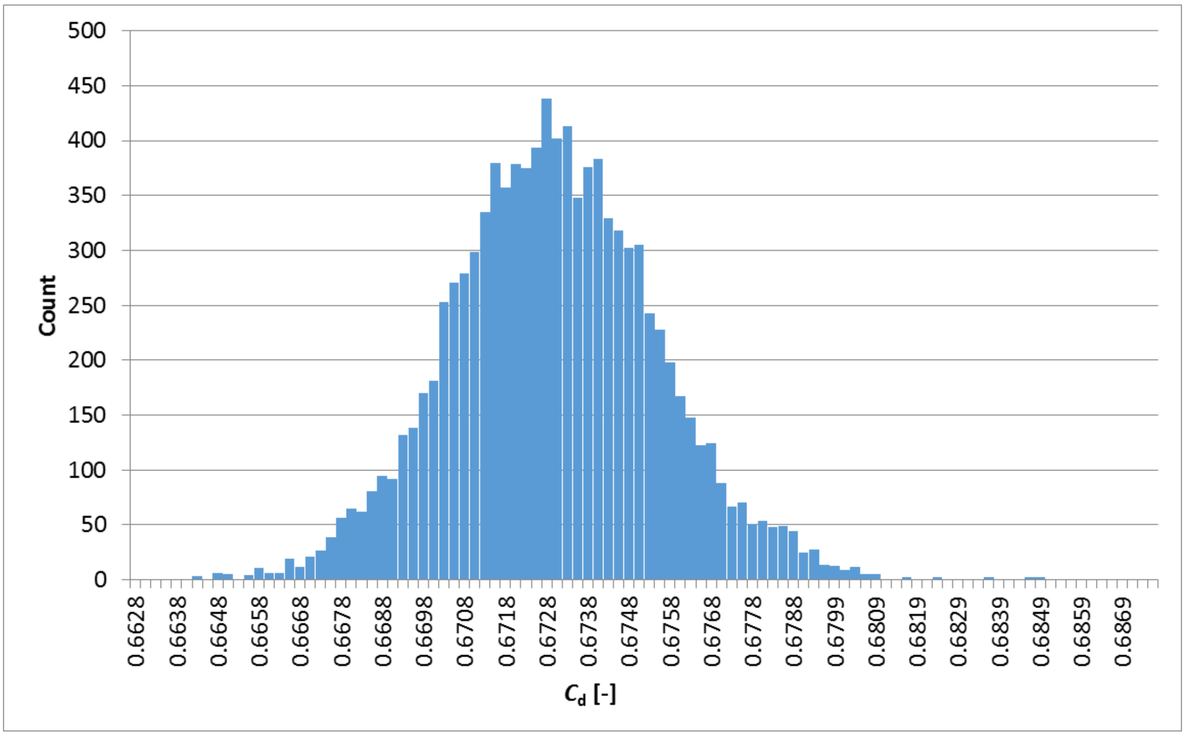

Fig. 6. A histogram of the observed values of the discharge coefficient $C_d = 0.673$.

The results of estimating the expanded uncertainties $U_p(C_d)$ for all measuring points of discharge coefficient C_d are summarized in Table 4 in the following convention: $(\overline{C_d} \pm U_p(C_d))$ [-].

Table 4. The results of discharge coefficient estimation from GUM and Monte Carlo method.

Discharge coefficient estimation 10^{-2}[-]	
GUM method	**MC method**
(67.30±0.50)	(67.31±0.51)
(70.68±0.60)	(70.68±0.62)
(74.34±0.67)	(74.31±0.66)
(78.44±0.71)	(78.40±0.72)
(83.51±0.83)	(83.49±0.85)

Figure 7 presents the expanded uncertainties $U_p(C_d)$ of the discharge coefficient C_d obtained by GUM and Monte Carlo simulation.

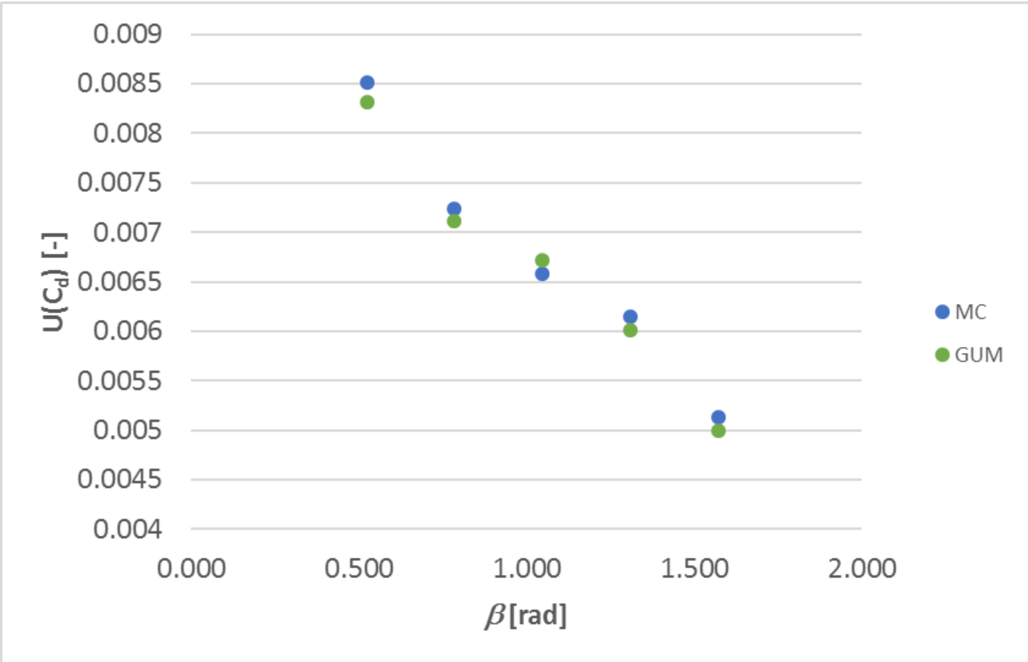

Fig. 7. The expanded uncertainty $U_p(C_d)$.

Figure 8 shows the relative expanded uncertainties $\delta U_p(C_d)$ (determined from the formula (21)):

$$\delta U_p(C_d) = \frac{U_p(C_d)}{C_d} \cdot 100\% \tag{22}$$

of the discharge coefficient C_d from GUM and Monte Carlo method.

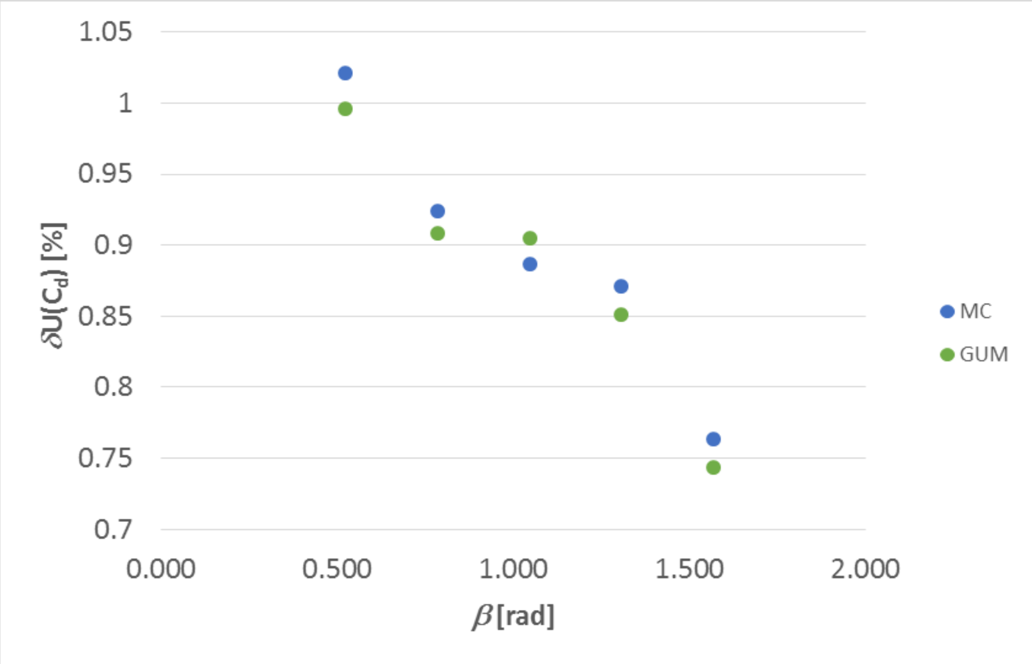

Fig. 8. The relative expanded uncertainty $\delta U_p(C_d)$.

From Figures 7 and 8, it can be seen that there is a strong correlation between the measurement uncertainty of the discharge coefficient C_d in relation to the angle β of the oblique weir for both analytically determined results and the Monte Carlo method.

It can be seen that all estimated values of the C_d measurement uncertainty decrease as the angle increases. This means that C_d is inversely proportional to the weir angle on the dive side in all cases.

The comparison between actual (the experimental value) C_d and that values calculated using equation (10) (MLR) and both GUM and MC methods was shown in Fig. 9.

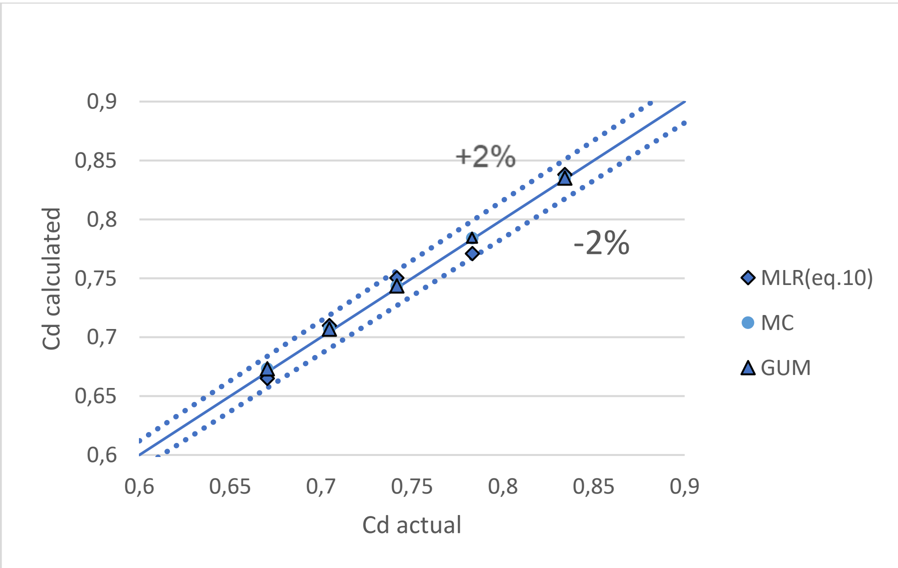

Fig. 9. The comparison between C_d actual and theoretical data calculated and that values measured from GUM and MC method.

It can be seen that C_d actual values are agreed with theoretical values with the relative error does not exceed ±2%.

5. **Conclusion**:

The paper presents step by step methodology for estimating uncertainty of the discharge coefficient C_d for a side weir, considering a specific case. Which is very important, because there has not been a compact procedure in the literature to estimate the measurement uncertainty of the discharge coefficient C_d.

The methodology for estimating measurement uncertainty presented in the article can be helpful during research on the construction and parameters of hydraulic structures and hydraulic measurements. In the article, the authors determined the value of uncertainty distributed both by the method consistent with GUM recommendations and the Monte Carlo method. The test results obtained by both methods are convergent and show that the maximum uncertainty value (for the analyzed experiment) $U_p(C_d)$ is equal to 0.0085, occurs for the smallest tested $\beta = 0.5$ rad. However, the relative expanded uncertainty $U_p(C_d)$ of the discharge coefficient C_d does not exceed 1.02%.

The analyzes also proved that is a strong correlation (inversely proportional) between the measurement uncertainty of the discharge coefficient C_d in relation to the angle β of the oblique weir.

Notations:

Symbol	***Meaning***	***Dimensions***
C_d	coefficient of discharge	-
F_3	Froude number in the side channel	-
y_3	water depth at side channel	L
y_1	up stream main channel	L
L	the length of the side weir crest	L
b	the width of side channel	L
p	the height of side weir	L
Q_1	discharge up a stream side channel	L^3T^{-1}
Q_2	discharge downstream side channel	L^3T^{-1}
Q_3	discharge in the side channel	L^3T^{-1}
F_1	Froude number in the main channel	-
V_1	The velocity of flow in the main channel	LT^{-1}
β	the angle of oblique side weir	rad
E	specific energy	L
y	water depth	L

v	mean velocity	LT^{-1}
g	acceleration due to gravity	LT^{-2}
Q	flow discharge	L^3T^{-1}
A	cross section area of flow	L^2
x	distance along channel	L
μ	dynamic viscosity of water	MLT^{-2}
ρ	density of water	ML^{-3}
R	Reynold's number	-
n	number of C_d measurements,	-
C_{di}	the measured C_d value for i =1, 2, …n,	-
$\overline{C_d}$	C_d arithmetic mean value.	-
c_0 to c_5	marks sensitivity coefficients	-

References

[1] G. De Marchi, Essay on the Performance of Lateral Weirs, L Energia Electrica Milano, vol. 11, No. 11, Italy, 1934, pp. 849–860.

[2] A. El-Khashab, K.V.H. Smith, Experimental investigation of flow over side weirs, J. Hydraul. Div. 102 (9) (1976) 1255–1268.

[3] M.E. Emiroglu, H. Agaccioglu, N. Kaya, Discharging capacity of rectangular side weirs in straight open channels, Flow Meas. Instrum. 22 (2011) 319–330.

[4] M.E. Emiroglu, N. Kaya, H. Agaccioglu, Closure to "Discharge capacity of labyrinth side weir located on a straight channel by M. Emin Emiroglu, Nihat Kaya, and Hayrullah Agaccioglu", J. Irrig. Drain. Eng. (2011) 745–746, dx.doi.org/10.1061 / (ASCE)IR .1943-4774.0000350.

[5] K.G. Ranga Raju, B. Prasad, S.K. Gupta, Side weirs in rectangular channels, J. Hydraul. Div. ASCE 105 (1979) 547–554.

[6] K. Subramanya, S.C. Awasthy, Spatially varied flow over side weirs, J. Hydraul. Div. ASCE 98 (1972) 1–10.

[7] A. Uyumaz, Y. Muslu, Flow over side weirs in circular channels, J. Hydraul. Div. ASCE 111 (1985) 144–160.

[8] S.M. Borghei, M.R. Jalili, M. Ghodsian, Discharge coefficient for sharp-crested side weirs in subcritical flow, J. Hydraul. Eng. ASCE 125 (1999) 1051–1056.

[9] A. Vatankhah, Analytical solution for water surface profile along a side weir in a triangular channel, Flow Meas. Instrum. 23 (1) (2012) 76–79.

[10] A. Vatankhah, New solution method for water surface profile along a side weir in a circular channel, J. Irrig. Drain. Eng. (2012) 948–954, http://dx.doi.org/10.1061/(ASCE)IR.1943-4774.0000483.

[11] H.M. Azamathulla, A.H. Haghiabi, A. Parsaie, Prediction of side weir discharge coefficient by support vector machine technique, Water Sci. Technol. 16 (4) (2016) 1002–1016.
[12] A.M.M. El-Khashab, Hydraulics of Flow Over Side Weirs (Ph.D. thesis), University of Southampton, England, 1975.
[13] W.H. Hager, Lateral outflow of side weirs, J. Hydraul. Eng. ASCE 113 (1987) 491–504.
[14] R. Singh, D. Manivannan, T. Satyanarayana, Discharge coefficient of rectangular side weirs, J. Irrig. Drain. Eng. ASCE 120 (1994) 814–819.
[15] M.R. Jalili, S.M. Borghei, Discussion of Discharge coefficient of rectangular side weir, by Singh, R., Manivannan, D., Satyanarayana, J. Irrig. Drain. Eng. ASCE 122 (1996) 132.
[16] Mwafaq Y. Mohammed, Ahmed Y. Mohammed. Discharge coefficient for an inclined side weir crest using a constant energy approach, Flow Measurement and Instrumentation, Vol. 22, 2011, pp. 495-499.
[17] Ahmed Y Mohammed. "theoretical Analysis of flow over the side weir using Runge Kutta Method" international Journal of Engineering, 2011 IX (2),47-50.
[18] Ahmed Y Mohammed. "Numerical Analysis of Flow over side weir" Journal of King Saud UniversityEng.Sci, 2015. 27,37-42, https://doi.org/10.1016/j.jksues.2013.03.004
[19] Ahmed Y Mohammed, Azza N. Altalib and Talal A. Basheer. Simulation of Flow Over The Side Weir Using Simulink. Scientia Iranica.; 2013. 20 (4):1094–100.
[20] Azza N. AL-Talib, Flow over oblique side weir, Damascus Univ. J. 28 (1) (2012) 15–22.
[21] Isa E.,Hossein B.,Amir Hossein B.,Hamed A.and Ali Sh. ."Gene expression programming to predict the discharge coefficient in rectangular side weir." Applied soft computing 2015, 35,618-628.
[22] R. Singh, D. Manivannan, T. Satyanarayana, Discharge coefficient of rectangular side weirs, J. Irrig. Drain. Eng. ASCE 120 (1994) 814–819.
[23] Guide to the Expression of Uncertainty in Measurement, JCGM 100 :2008.
[24] J. Taylor, Introduction to error analysis the study of uncertainties in physical measurements, second edition, University Science Books, New York, 1997.
[25] Supplement 1 to the Guide to the expression of uncertainty in measurement – Propagation of distributions using a Monte Carlo method, (JCGM 101:2008).
[26] A. Dzwonkowski, A. Golijanek-Jędrzejczyk, Estimation of the uncertainty of the AC/AC transducer output voltage, Przegl. Elektrotech. 91(10) (2015), 166-169, DOI: 10.15199/48.2015.10.3.
[27] A. Dzwonkowski, L. Swędrowski, Uncertainty analysis of measuring system for instantaneous power research, Metrol. Meas. Syst. 19(3) (2012), 573-582.
[28] A. Golijanek-Jędrzejczyk, D. Świsulski, R. Hanus, M. Zych, L. Petryka, Flow Measurement and Instrumentation 62, 84-92 (2018)
[29] Roshani G.H., Hanus R., Khazaei A., Zych M., Nazemi E., Mosorov V.: Density and velocity determination for single-phase flow based on radiotracer technique and neural networks. Flow Measurement and Instrumentation, Vol. 61 (2018), pp. 9–14. DOI: https://doi.org/10.1016/j.flowmeasinst.2018.03.006
[30] J. Le Coz, B. Renard, L. Bonnifait, F. Branger, R. Le Boursicaud. Combining hydraulic knowledge and uncertain gaugings in the estimation of hydrometric rating curves: a Bayesian approach. Journal of Hydrology, Elsevier, 2014, 509, p. 573 - p. 587. <10.1016/j.jhydrol.2013.11.016>. <hal-00934237>

[31] J. Sau, P.Malaterre, J.Baume, Sequential Monte Carlo hydraulic state estimation of an irrigation canal, Comptes Rendus Mécanique, Volume 338, Issue 4, 2010, Pages 212-219, ISSN 1631-0721, https://doi.org/10.1016/j.crme.2010.03.013.

[32] M. Rohaninejad, M. Zarghami, Combining Monte Carlo and finite difference methods for effective simulation of dam behavior, Advances in Engineering Software, Vol.45, Issue 1, 2012, Pages 197-202, https://doi.org/10.1016/j.advengsoft.2011.09.023

[33] Papalaskaris, T.; Panagiotidis, T. Forecasting Low Stream Flow Rate Using Monte—Carlo Simulation of Perigiali Stream, Kavala City, NE Greece. *Proceedings* **2018**, *2*, 580.